

Nonlinear splitting of magnetoelastic resonance line in powerfully excited ferrite

© V.S. Vlasov,¹ V.G. Shavrov,² V.I. Shcheglov²

¹ Syktyvkar State University, Syktyvkar, Russia

² Kotelnikov Institute of Radio Engineering and Electronics, Russian Academy of Sciences, Moscow, Russia

e-mail: vshcheg@cplire.ru

Received June 1, 2021

Revised August 31, 2021

Accepted September 1, 2021

The nonlinear splitting of magnetoelastic resonance line in powerfully excited ferrite is investigated. It is shown that the amplitude of split resonance has the same order of value that the amplitude of basis resonance and its frequency is determined by the upper boundary of nonlinear amplitude-frequency characteristic of magnetic system. It is found the threshold character of splitting additional resonance from general. It is determined the possibility of operation of split elastic resonance frequency by changing of excited magnetic field value which has practical importance.

Keywords: ferromagnetic resonance, magnetoelastic interaction, nonlinear vibrations.

DOI: 10.21883/TP.2022.01.52531.167-21

Introduction

High-power ultrasonic vibrations excited by magnetostrictive transducers find numerous applications in different branches of technology [1,2]. The excitation of hypersonic vibrations at frequencies up to 10 GHz (and above) is of special interest. The use of magnetoacoustic resonance is rather promising in this regard [3–5]. Garnet ferrite films open up additional opportunities for significant broadening of the frequency range of transducers through the excitation of up to several hundred elastic modes over the thickness of the film–substrate structure [6]. The power of excitation of hypersonic in such transducers is limited to several tens of milliwatts. This is attributable to the parametric excitation of exchange spin waves, which induces strong absorption of the incoming signal after a certain threshold is exceeded [7–9]. This excitation may be prevented by using a normally magnetized thin ferrite disk as a working medium of a transducer. The frequency of ferromagnetic resonance in such a geometry is at the bottom of the spectrum of exchange waves. As a result, the excitation of these waves is inhibited [10–12]. Such conditions were implemented in [13–16], and the possibility to raise the level of excitation of hypersonic by 2–3 orders of magnitude or more was demonstrated.

However, little attention was paid in these studies to the amplitude-frequency properties of the nonlinear resonance of the magnetic system and to the dissipation of the elastic system. This prevents one from realizing fully the potential of high level of excitation.

The present study is a more detailed examination of the resonance frequency properties of both systems aimed at

revealing additional opportunities for generation of high-power hypersonic.

1. Geometry of the problem and main equations

Figure 1 illustrates the overall geometry of the problem [13–16]. Fundamental to it is a ferrite plate with thickness d magnetized along a normal to its surface.

We assume that ferrite is isotropic in magnetic properties and features cubic symmetry in elastic and magnetoelastic properties. The planes of the cube face and the ferrite plate correspond to each other. Plane Oxy of Cartesian coordinate system $Oxyz$ is aligned with the plate plane. The external field is $\mathbf{H} = \{h_x; h_y; H_0\}$, where H_0 is a constant bias field and $h_{x,y}$ are components of a variable field. When shear elastic vibrations are excited along axis Oz (i.e., at $u_z = 0$ and $\partial/\partial(x, y) \rightarrow 0$), the elastic and magnetoelastic

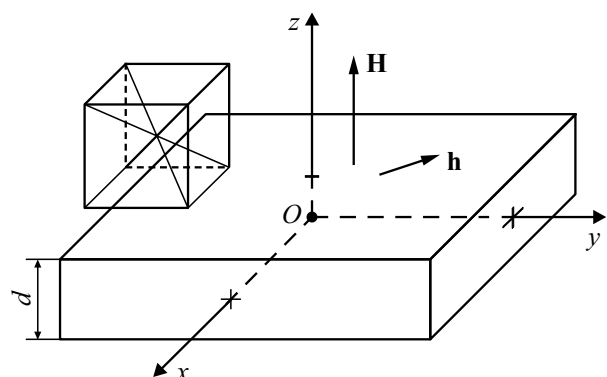


Figure 1. Geometry of the problem.

properties of the medium are characterized by constants c_{44} and B_2 , respectively.

The equation of motion for magnetization component m_x takes the form

$$\frac{\partial m_x}{\partial t} = -\frac{\gamma}{1+\alpha^2} [(m_y + \alpha m_x m_z) H_{ez} - (m_z - \alpha m_y m_x) H_{ey} - \alpha(m_y^2 + m_z^2) H_{ex}], \quad (1)$$

and the equations for m_y and m_z are derived from (1) by cyclic interchange of x, y, z . Here, $\mathbf{m} = \mathbf{M}/M_0$ is the normalized magnetization vector, M_0 is the saturation magnetization, and α is the Gilbert damping constant.

The effective fields in these equations take the form

$$H_{ex} = h_x + H_{ax}, \quad (2)$$

$$H_{ey} = h_y + H_{ay}, \quad (3)$$

$$H_{ez} = H_0 - 4\pi M_0 m_z + H_{az}, \quad (4)$$

where

$$H_{ax} = -\frac{B_2}{M_0} m_z \frac{\partial u_x}{\partial z}, \quad (5)$$

where u_x is the elastic displacement component and H_{ay} and H_{az} are derived from (5) by cyclic interchange of x, y, z .

The equation for displacement component u_x has the form

$$\frac{\partial^2 u_x}{\partial t^2} + 2\beta \frac{\partial u_x}{\partial t} - \frac{c_{44}}{\rho} \frac{\partial^2 u_x}{\partial z^2} = 0, \quad (6)$$

and the equation for u_y is derived from (6) by substituting x with y .

The boundary conditions for displacement component u_x at free plate surfaces have the form

$$c_{44} \frac{\partial u_x}{\partial z} \Big|_{z=\pm d/2} = -B_2 m_x m_z, \quad (7)$$

and the conditions for u_y are derived from (7) by substituting x with y .

In the present study, the variable field is assumed to be sinusoidal with right-hand circular polarization:

$$h_x = h_0 \sin(2\pi f t), \quad (8)$$

$$h_y = -h_0 \cos(2\pi f t), \quad (9)$$

where h_0 is the excitation amplitude.

Solving the system of Eqs. (1)–(6) with boundary conditions (7) using the Runge–Kutta method (as it was done in [13–16]), one may determine the temporal evolution and the frequency characteristics of magnetic and elastic vibrations excited by the variable field.

Material parameters typical for single crystals of yttrium iron garnet (YIG) were used in calculations in the present study: $4\pi M_0 = 1750$ Gs, $B_2(\text{YIG}) = 6.96 \cdot 10^5$ J/m³, $c_{44} = 7.64 \cdot 10^{10}$ J/m³. The damping (Gilbert) parameter of the magnetic subsystem was $\alpha = 0.02$. The values of

damping parameter of the elastic subsystem β were chosen from the 10^6 – 10^9 s^{−1} interval, and the value of $\beta = 0$ s^{−1} was used additionally as a reference. The other parameters were chosen so that the resonance frequencies of uniform precession and the first mode of elastic vibrations were both equal to 2800 MHz with no magnetoelastic coupling in the case of linear vibrations. The constant field was $H_0 = 2750$ Oe, and the thickness of the magnetic plate was $0.06865 \cdot 10^{-6}$ m. The amplitude of the variable field was $h_0 = 0.01$ Oe and 10 Oe in linear and nonlinear modes, respectively.

2. Frequency characteristics of nonlinear magnetoelastic vibrations

In accordance with the formulation of the problem, vibrations are excited in the complete magnetoelastic system by applying a variable field to the magnetic subsystem. Therefore, we first consider how the elastic subsystem manifests itself in this case.

Let us turn to Fig. 2 where the frequency characteristics of the amplitude of magnetic (a) and elastic (b) vibrations at different levels of coupling between the magnetic and elastic systems are presented. Since this coupling is due to the magnetoelastic interaction, we examine the characteristics at two different values of the magnetoelastic coupling constant: one corresponding to YIG (curves 1) and another one that is five times lower (curves 2). In the first case, the coupling is typical of the experimental conditions, while the coupling in the second case is almost nonexistent (although still sufficient to excite vibrations in the elastic system).

Let us examine the case of weak coupling first (curves 2). The nonlinear resonance characteristic seen in Fig. 2, a has the typical shape of a triangle skewed toward higher frequencies due to the detuning mechanism with a maximum near 3.02 GHz. It follows from Fig. 2, b that the frequency characteristic of elastic vibrations in this case is symmetrical with a central maximum at the resonance frequency of natural elastic vibrations of the plate (2.8 GHz). The high-frequency peak of magnetic resonance (curve 2 in Fig. 2, a) has almost no effect on elastic vibrations (curve 2 in Fig. 2, b). The magnetic characteristic has a notch in the region of elastic resonance (2.8 GHz), but this notch is rather insignificant.

In the case of strong coupling (curves 1), both characteristics change substantially. The magnetic characteristic (curve 1 in Fig. 2, a) exhibits first an upward spike and then a downward spike in the region of elastic resonance (2.8 GHz), and the characteristic itself rises up by more than 20% in the region from 2.94 to 3.02 GHz. The primary peak of the elastic characteristic is amplified significantly (approximately by a factor of 2) and shifts downward slightly (from 2.89 to 2.78 GHz), and a strong additional resonance rise with a magnitude of almost 50% of the primary peak emerges in the region from 2.94 to 3.02 GHz. This rise has the shape of a „split-off“ from the primary peak

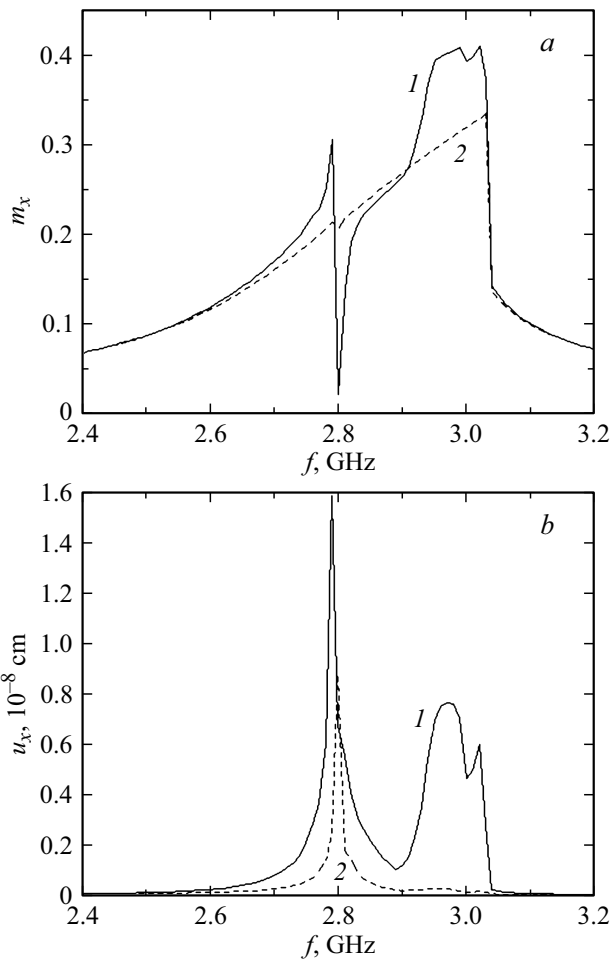


Figure 2. Frequency characteristics of the amplitude of magnetic (a) and elastic (b) vibrations at different values of the magnetoelastic interaction constant: 1 — $B_2 = B_2(\text{YIG})$, 2 — $B_2 = 0.2B_2(\text{YIG})$.

and corresponds to the rise of the magnetic characteristic (i.e., is located in the region of influence of the detuning mechanism). Note that this rise is not integral: in its high-frequency part, a relatively small second additional rise corresponding in frequency to the high-frequency cutoff of the magnetic characteristic (3.02 GHz) is apparent.

3. Influence of the excitation level on the elastic resonance parameters

Let us consider the dependences of the frequency and the amplitude of the first and the second additional resonances on the excitation level (see Figs. 3 and 4).

Figure 3 shows the dependences of the frequency of the primary rise 1 and the first 2 and the second 3 additional rises of the frequency characteristic of the amplitude of elastic displacement on the excitation amplitude.

It can be seen that the primary rise, which corresponds to the frequency of partial resonance of the elastic system

(2.8 GHz, curve 1), persists at all levels of excitation. Its frequency is almost independent of the excitation amplitude.

The first additional resonance (curve 2) emerges at an excitation level exceeding 4 Oe and persists at all higher excitation levels. The frequency of this resonance depends linearly on the excitation amplitude with a slope ratio of 0.0124 GHz/Oe. The second additional resonance (curve 3) exists only at excitation levels falling within the interval from 9 to 32 Oe. Its frequency also depends linearly on the excitation amplitude with the same slope ratio, but lies 0.06 GHz higher than the frequency of the first additional resonance.

Figure 4 shows the dependences of the amplitude of the primary resonance and the first and the second additional

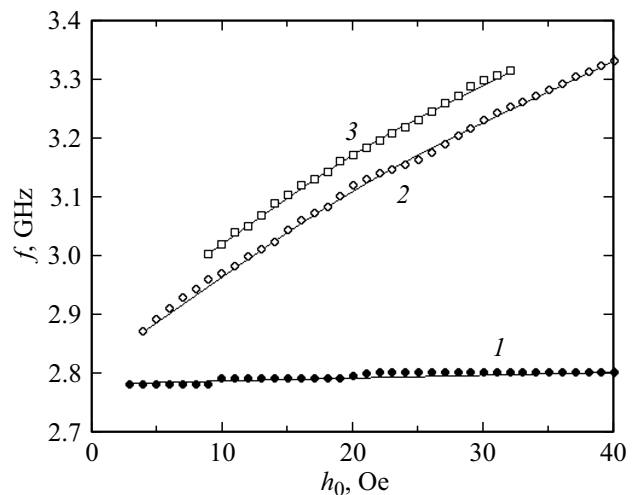


Figure 3. Dependences of the frequency of the primary resonance (1) and the first (2) and the second (3) additional resonances of the frequency characteristic of elastic displacement on the excitation amplitude.

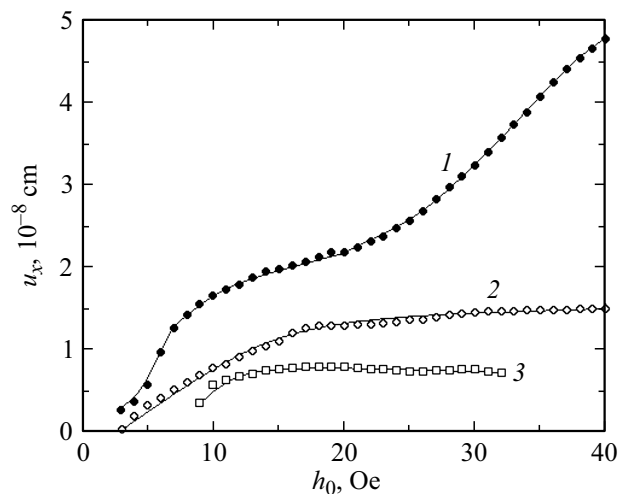


Figure 4. Dependences of the amplitude of the primary resonance (1) and the first (2) and the second (3) additional resonances of the frequency characteristic of elastic displacement on the excitation amplitude.

resonances of the frequency characteristic of elastic displacement on the excitation amplitude.

It can be seen that the primary rise, which corresponds to the frequency of partial resonance of the elastic system (2.8 GHz, curve 1), becomes more prominent as the levels of excitation increases. At excitation amplitudes below 8 Oe, the magnitude of this rise increases fairly rapidly, but its growth slows down as the excitation amplitude increases further to approximately 25 Oe. This is attributable to the partial transfer of energy of the system from the primary resonance to additional resonances. As the excitation level crosses the threshold of 25 Oe, the magnitude once again starts increasing rapidly (apparently, due to the restrictions on the energy transfer to additional resonances). The amplitude of the first additional resonance (curve 2) also increases at first, but starts saturating at approximately 17 Oe and remains almost constant at higher excitation levels. The amplitude of the first additional resonance in the excitation interval of 3–25 Oe (i.e., up to pronounced saturation) is approximately two times lower than the amplitude of the primary resonance in the same interval. The amplitude of the second additional resonance (curve 3) also increases rapidly at first, but its growth soon reaches saturation at a level approximately two times lower than that of the amplitude of the first additional resonance. At excitation levels higher than 32 Oe, the second additional resonance, lacking its own pronounced peak, merges with the first one.

The results presented in this section may be regarded as a demonstration of feasibility of tuning of the frequency of elastic resonance in the interval from 2.86 to 3.32 GHz (i.e., within 15%) by varying the excitation level from 5 to 40 Oe. This opportunity to control the frequency of elastic resonance is likely to have certain applications in practice. This control technique has an important advantage in that it does not require altering the mechanical parameters of the system (specifically, the thickness of the ferrite plate).

4. Influence of the level of elastic dissipation

The results presented in the previous section were obtained at a specifically chosen relatively low level of elastic dissipation. This choice was made for the sake of clarity. Let us now consider the above phenomena in a wide interval of elastic dissipation.

Figure 5 demonstrates the dependences of the amplitude of the primary resonance and both additional resonances of the frequency characteristic of elastic displacement on the elastic dissipation parameter.

It can be seen that the amplitudes of all resonances decrease gradually as the dissipation parameter increases. The primary rise, which corresponds to the partial frequency of the elastic resonance of the plate (curve 1), remains fairly well-pronounced within the entire examined interval

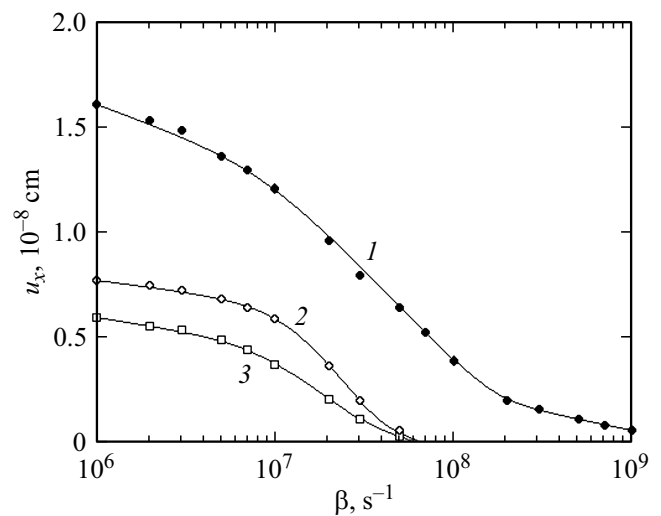


Figure 5. Dependences of the amplitude of the primary resonance (1) and the first (2) and the second (3) additional resonances of the frequency characteristic of elastic displacement on the elastic dissipation parameter. The horizontal axis is logarithmic in scale.

of variation of parameter β (from 10^6 to 10^9 s^{-1}), but its magnitude decreases approximately by a factor of 20. Although the resonance rise broadens in frequency, retains its distinctive character (i.e., the shape of a central maximum with downward slopes at both sides). As the dissipation parameter increases further (not shown), the resonance becomes aperiodic: it replicates the triangular skewed (toward higher frequencies) shape of the magnetic resonance with a decreasing amplitude.

The amplitudes of both additional resonances (curves 2 and 3) also decrease as the dissipation parameter increases, but the side resonances merge with the primary one at β approximately equal to $5 \cdot 10^7 \text{ s}^{-1}$. Thus, the first and the second additional resonances may be distinguished clearly only if the dissipation parameter is lower than $5 \cdot 10^7 \text{ s}^{-1}$. If magnetic dissipation parameter α decreases by a factor of 4 (from 0.020 to 0.005), the additional resonances merge with each other, although the critical value of $\beta = 5 \cdot 10^7 \text{ s}^{-1}$ at which they merge with the primary resonance remains almost unchanged.

The results of a control check demonstrate that if dissipation parameter β drops below 10^6 s^{-1} down to zero (not shown in Fig. 5), the amplitude of resonances remains limited at $1.7 \cdot 10^{-8} \text{ cm}$ (the primary resonance), $0.8 \cdot 10^{-8} \text{ cm}$ (the first additional resonance), and $0.6 \cdot 10^{-8} \text{ cm}$ (the second additional resonance).

Thus, a sufficiently small value of the elastic dissipation parameter is a prerequisite for implementing excitation-level control over an elastic resonance. In the present case, β needs to be below $5 \cdot 10^7 \text{ s}^{-1}$, which is perfectly feasible for YIG [3,4].

5. Temporal evolution of vibrations

Since the elastic resonance is split in the strongly nonlinear mode, it is of some interest to examine the temporal evolution of vibrations.

Let us turn to Fig. 6 where the temporal evolution of vibrations occurring after the application of magnetic excitation is presented. Two frequencies were considered. The first one corresponds to the primary frequency of elastic resonance (2.80 GHz), and the second one is the central frequency of the dominant additional resonance of elastic vibrations (2.97 GHz).

It can be seen from Figs. 6, *a* and 6, *c* that the amplitude of magnetic vibrations (Fig. 6, *a*) increases sharply right after the application of excitation, since the excitation energy needs more time to reach the elastic system with its amplitude of vibrations (Fig. 6, *b*) increasing much more slowly. The amplitude of magnetic vibrations then decreases gradually, while the amplitude of elastic vibrations increases.

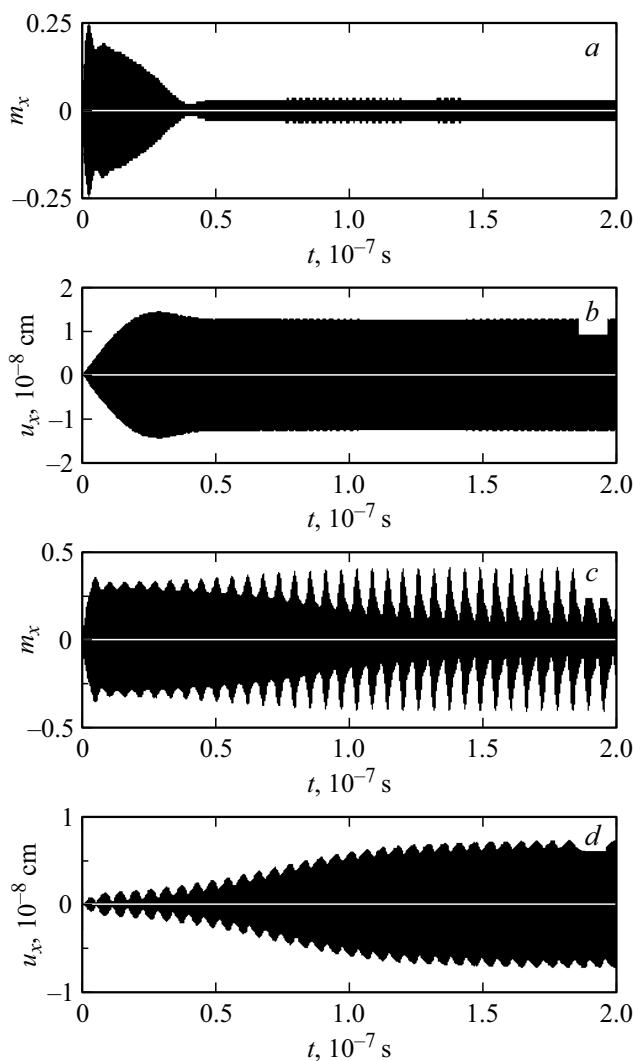


Figure 6. Temporal evolution of magnetic (*a, c*) and elastic (*b, d*) vibrations at different frequencies: *a, b* — 2.80 GHz (primary resonance); *c, d* — 2.97 GHz (first additional resonance).

This corresponds to the transfer of energy from the magnetic system to the elastic one. After about $0.5 \cdot 10^{-7}$ s, an energy balance is established and the amplitudes of vibrations in both systems reach steady levels. This pattern corresponds to the usual excitation of vibrations in a system of two coupled oscillators and remains like this in the linear mode.

The same, however, is not true for the frequency of the additional resonance of the elastic system. It can be seen from Fig. 6, *c* that magnetic vibrations here also increase sharply at first, but the excitation of elastic vibrations (i.e., the transfer of energy from the magnetic system to the elastic one) proceeds much more slowly (Fig. 6, *d*) than in the previous case. As a result, the steady-state mode of both vibrations is established only at approximately $1.5 \cdot 10^{-7}$ s (i.e., three times later than at the frequency of the primary resonance). This greatly delayed excitation of elastic vibrations is likely associated with the fact that the excitation frequency (2.97 GHz) shifts away from the frequency of natural vibrations of the elastic system (2.80 GHz). In other words, strong magnetic vibrations force the elastic system to vibrate at an unnatural frequency, and it demonstrates a certain resistance. The amplitude of both magnetic and elastic vibrations is highly jagged in nature due to beats. The beats period is approximately $5.7 \cdot 10^{-9}$ s. This corresponds to a frequency of 0.17 GHz that is the difference between the excitation frequency and the frequency of the primary resonance, as is typical of forced vibrations.

Concluding remarks

The main result of this study is arguably the demonstration of splitting of the elastic resonance in the case of strongly nonlinear excitation of the magnetic system. This splitting is manifested in the emergence of two additional resonances at separate frequencies. The threshold nature of splitting was established. It was found that the maximum additional resonance is comparable in amplitude to the primary one, while its frequency is defined by the upper frequency of the nonlinear frequency characteristic of the magnetic system. The potential to control the frequency of the additional elastic resonance by varying the level of magnetic excitation was demonstrated. The practical relevance of this control method, which does not require altering the mechanical parameters of the system, was noted.

Funding

The work has been performed under the state assignment and supported in part by grants from the Government of the Komi Republic and the Russian Foundation for Basic Research (No. 20-42-110004, r_a) and the Russian Science Foundation (No. 21-72-20048).

Conflict of interest

The authors declare that they have no conflict of interest.

References

- [1] I.P. Golyamina, in *Ul'trazvuk. Malen'kaya entsiklopediya* (Sovetskaya Entsiklopediya, M., 1979), p. 196–200 (in Russian).
- [2] I.P. Golyamina, in *Fizika i tekhnika moshchnogo ul'trazvuka. Kniga 1. Istochniki moshchnogo ul'trazvuka*, ed. I.P. Golyamina (Nauka, M., 1967) (in Russian).
- [3] R.L. Comstock, R.C. LeCraw. *J. Appl. Phys.*, **34** (10), 3022 (1963).
- [4] R.C. LeCraw, R.L. Comstock, in book: *Physical Acoustics. V. 3. Part B. Lattice Dynamics* (Academic Press, NY and London, 1965), p. 156.
- [5] E. Schlömann, R.I. Joseph. *J. Appl. Phys.*, **35** (8), 2382 (1964).
- [6] S.N. Polulyakh, V.N. Bershansky, E.Yu. Semuk, V.I. Belotelov, P.M. Vetoshko, V.V. Popov, A.N. Shaposhnikov, A.I. Chernov. *Journ. Tech. Phys.*, **21**(7), 1124 (2021).
- [7] A. Gurevich, G. Melkov. *Magnetic Oscillations and Waves* (Nauka-Fizmatlit, M., 1994)
- [8] Ya.A. Monosov, *Nelineynyi ferromagnitnyi rezonans* (Nauka, M., 1971) (in Russian).
- [9] V.S. L'vov, *Nelineynye spinovye volny* (Nauka, M., 1987) (in Russian).
- [10] Yu.V. Gulyaev, P.E. Zil'berman, A.G. Temiryazev, M.P. Tikhomirova, *Phys. Solid State*, **42** (6), 1094 (2000).
- [11] D.I. Sementsov, A.M. Shutyi, *Phys.-Usp.*, **50** (8), 793 (2007).
- [12] Th. Gerrits, M.I. Schneider, A.B. Kos, T.J. Silva. *Phys. Rev. B*, **73** (9), 094454(7) (2006).
- [13] V.S. Vlasov, L.N. Kotov, V.G. Shavrov, V.I. Shcheglov, *J. Commun. Technol. Electron.*, **54** (7), 821 (2009).
- [14] V.S. Vlasov, V.G. Shavrov, V.I. Shcheglov, *Zh. Radioelektron.*, (2) (2013) (in Russian).
<http://jre.cplire.ru/jre/feb13/10/text.pdf>
- [15] V.S. Vlasov, P.A. Makarov, V.G. Shavrov, V.I. Shcheglov, *Zh. Radioelektron.*, (6) (2017) (in Russian).
<http://jre.cplire.ru/jre/jun17/5/text.pdf>
- [16] F.F. Asadullin, S.M. Poleshchikov, D.A. Pleshev, L.N. Kotov, V.V. Vlasov, V.G. Shavrov, V.I. Shcheglov. *J. Siberian University. Mathematics and Physics*, **10** (1), 36, (2017).